Single-focus binary Fresnel zone plate

Francisco Jose Torcal-Milla[a,1], Luis Miguel Sanchez-Brea[b]

[a]*Applied Physics Department, Universidad de Zaragoza, 50009, Zaragoza (Spain).*
[b]*Applied Optics Complutense Group, Optics Department, Facultad de Ciencias Fisicas,Universidad Complutense de Madrid, Plaza de las Ciencias 1, 28040, Madrid (Spain)*

Abstract

In this work, we propose and analyze a novel kind of binary Fresnel zone plate with single focus. It consists of a Fresnel zone plate whose zones have rough edges. We give analytical results for the intensity along the optical axis and demonstrate that lateral roughness of the zones produces the disappearance of secondary foci as a blurring of the edges. Besides, we corroborate its behavior by numerical simulations and experiments. This kind of Fresnel zone plate can be useful in a wide range of photonic applications, even for focusing with soft and hard X-rays or extreme ultraviolet radiation.

Keywords: electromagnetic diffraction, Fresnel zone plate, statistical optics
PACS: 42.79.Ci, 42.25.Fx, 42.25.Bs

1. Introduction

Fresnel zone plates (FZPs) are optical diffractive elements that concentrate the light in a similar fashion as a conventional refractive lens. It results in a number of concentric annular zones which act somehow like a refractive lens but with some additional diffracting effects due to the edges between zones. The dimensions of the zones are based on the Fresnel zone concept [1]. FZPs have been analyzed from several points of view and performances, [2, 3, 4, 5, 6]. It appears as a fundamental part in applications such as spectroscopy, nanolithography, near-field and far-field optical microscopy, or optical antennas, [7, 8, 9, 10, 11, 12], involving also X-rays [13, 14] and extreme-ultraviolet radiation. The zones of FZPs have blazed profiles for an optimal performance, but binary phase or amplitude FZPs are also possible, being easier in manufacturing, [15]. Although, due to diffractive effects, binary FZPs present secondary foci that worsen the behavior of the lens. Some research has been developed in this sense. In [16] the authors demonstrate that secondary foci can be suppressed by several orders of

---

Email address: `fjtorcal@unizar.es` (Francisco Jose Torcal-Milla)
[1]This work was started while F.J. Torcal-Milla was with the Optics Department, Universidad Complutense de Madrid, Madrid (Spain).

magnitude using a photon sieve. On the other side, in [17, 18] secondary foci are suppressed by using a Gabor Zone plate. In this work, we present and analyze the behavior of a kind of binary amplitude FZP whose zones edges present a certain random roughness that cancels secondary foci of the FZP. We obtain analytical equations describing the cancellation of secondary foci in terms of the roughness of the rings edges. Following, we corroborate the theoretical formalism by numerical simulations and experiments, finding a great agreement between them. As a comment, it is important to notice that the presented formalism is also valid for binary phase FZPs.

2. Theoretical approach

Firstly, let us consider a binary annular aperture without random roughness in the edges. By using the Fresnel approach for propagation, the field on axis after the annular aperture illuminated by a plane wave can be calculated as [1]

$$U_a = A_0 \frac{e^{ikz}}{ikz} \int_0^{2\pi} \int_{r_i}^{r_o} e^{i\frac{k\rho_0^2}{2z}} \rho_0 d\rho_0 d\theta, \tag{1}$$

where A_0 is the amplitude of the incoming beam, λ is the wavelength, z is the distance along the optical axis, r_i is the inner radio, and r_o is the outer radio of the aperture. Particularly, for a FZP the inner and outer radii of the annular apertures are approximately given by $r_{i,m} = \sqrt{(m-1)\lambda f}$ and $r_{o,m} = \sqrt{m\lambda f}$, respectively, being f the focal length of the desired FZP and m even numbers [1]. We may substitute these radii into Equation 1 and calculate the intensity diffracted by each annular aperture by multiplying by its complex conjugated. Thus, carrying out the summation over all apertures of the Fresnel zone plate, $m = 1, 2, ..., M$, the intensity along the optical axis produced by a FZP is given by

$$I(z) = \sum_{m,m'} U_{a,m} U_{a,m'}^* = A_0^2 \frac{sin^2\left(\frac{M\pi f}{z}\right)}{sin^2\left(\frac{\pi f}{z}\right)}, \tag{2}$$

where * means complex conjugated and M is the order of the last ring. Now, let us consider a certain random roughness in the radii of each annular aperture in the following way

$$U_a^r = A_0 \frac{e^{ikz}}{ikz} \int_0^{2\pi} \int_{r_i+\alpha_i}^{r_o+\alpha_o} e^{i\frac{k\rho_0^2}{2z}} \rho_0 d\rho_0 d\theta, \tag{3}$$

where α_i and α_o are unknown parameters that follow a certain random probabilistic distribution. The field calculated from Equation 3 results

$$U_a^r = \frac{2A_0\pi e^{ikz}}{k^2} \left[e^{i\frac{k(r_i+\alpha_i)^2}{2z}} - e^{i\frac{k(r_o+\alpha_o)^2}{2z}} \right]. \tag{4}$$
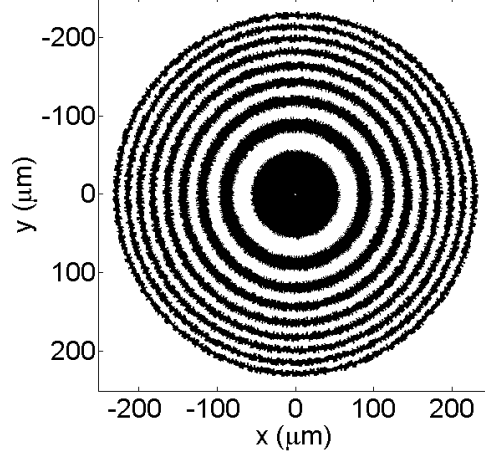
Figure 1: Fresnel zone plate with rough edges between zones and the following parameters: $D \approx 440 \ \mu m$, $\lambda = 630 \ nm$, $f = 5 \ mm$, $\sigma = 2 \ \mu m$ and $C = 0 \ \mu m$. σ and C define the roughness in the frontiers of the ring as we explain following.

Since α_i and α_o are given by random distributions, the intensity diffracted by an ensemble of concentric irregular rings can be expressed by using the corresponding joint probability density function, $p(\alpha)$, as [18]

$$
I^r = \int_{-\infty}^{\infty} \int_{-\infty}^{\infty} \left[\sum_{m,m'} U_{a,m}^r U_{a,m'}^{r*} p\left(\alpha_{i,m}, \alpha_{o,m}, \alpha_{i,m'}, \alpha_{o,m'}\right) \right]
$$
$$
\times d\alpha_{i,m} d\alpha_{o,m} d\alpha_{i,m'} d\alpha_{o,m'}. \tag{5}
$$

Thus, we have several random variables for each annular aperture into the intensity. An example of FZP of diameter D and rough zones edges is shown in Fig. 1.

Considering Gaussian distributions, the joint probability density function for each aperture is given by [18]

$$
p(\alpha) = \frac{1}{4\left(1 - C^2\right)\pi^2 \sigma^4}
$$
$$
\times e^{\frac{-\alpha_{i,m}^2 - \alpha_{i,m'}^2 + 2C\alpha_{i,m}\alpha_{i,m'} - \alpha_{o,m}^2 - \alpha_{o,m'}^2 + 2C\alpha_{o,m}\alpha_{o,m'}}{2(1-C)\sigma^2}}, \tag{6}
$$

where $\alpha = (\alpha_{i,m}, \alpha_{o,m}, \alpha_{i,m'}, \alpha_{o,m'})$, C is the correlation coefficient, $0 \leq C \leq 1$, and σ is the standard deviation of the radii with respect to the corresponding radii without roughness, [18, 19]. We consider that inner and outer radii are uncorrelated. Besides, we consider the same statistical parameters for all apertures. Then, summations in Equation 5 can be taken out of the integrals and

the intensity along the optical axis results

$$
\begin{aligned}
I^r(z) \;=\; A_0^2 \sum_{m,m'} \Bigg\{ & \frac{e^{\frac{ik\left(r_{i,m}^2-r_{i,m'}^2\right)z-k^2\left(r_{i,m}^2+r_{i,m'}^2-2Cr_{i,m}r_{i,m'}\right)\sigma^2}{2\left[z^2+(1-C^2)k^2\sigma^4\right]}}}{\sqrt{1+(1+C^2)\left(k\sigma^2/z\right)^2}} \\[2ex]
& +\frac{e^{\frac{ik\left(r_{o,m}^2-r_{o,m'}^2\right)z-k^2\left(r_{o,m}^2+r_{o,m'}^2-2Cr_{o,m}r_{o,m'}\right)\sigma^2}{2\left[z^2+(1-C^2)k^2\sigma^4\right]}}}{\sqrt{1+(1+C^2)\left(k\sigma^2/z\right)^2}} \\[2ex]
& -\frac{e^{\frac{ik\left(r_{i,m'}^2-r_{o,m}^2\right)z-k^2\left(r_{i,m'}^2+r_{o,m}^2\right)\sigma^2}{2\left[z^2+k^2\sigma^4\right]}}+e^{\frac{k}{2}\left(\frac{r_{o,m'}^2}{iz-k\sigma^2}-\frac{r_{i,m}^2}{iz+k\sigma^2}\right)}}{\sqrt{1+\left(k\sigma^2/z\right)^2}} \Bigg\}. \quad (7)
\end{aligned}
$$

The two first terms are formally equal and correspond to the inner and outer radii of each annular aperture. They depend on the correlation coefficient and the standard deviation of the random rough edges. On the other hand, the third and fourth terms do not depend on the correlation coefficient and, as simulations reveals, they are responsible of cancelling the secondary foci. In addition, a translation of the foci along axis due to the rough edges is also noticed. It is given by the term $\left(k\sigma^2/z\right)^2$ into the quotients of Equation 7. Now, performing the limit $\sigma \to 0$, we may recover the intensity distribution without randomness, Equation 2. On the other hand, performing the summations and using the definitions given before for the inner and outer radii of the different zones, being M the order of the last ring, Equation 7 simplifies to

$$
\begin{aligned}
I^r_{C=0}(z) \;=\; & \frac{A_0^2}{\sqrt{1+\left(k\sigma^2/z\right)^2}} e^{-\frac{2(M+1)\pi\,fk\sigma^2}{z^2+k^2\sigma^4}} \\[2ex]
& \times \frac{cos\left(\frac{2\pi Mf}{1+(k\sigma^2/z)^2}\right)-cosh\left(\frac{2\pi M\,fk\sigma^2}{z^2+k^2\sigma^4}\right)}{cos\left(\frac{2\pi f}{1+(k\sigma^2/z)^2}\right)-cosh\left(\frac{2\pi\,fk\sigma^2}{z^2+k^2\sigma^4}\right)} \\[2ex]
& \times \Bigg[\left(1-e^{\frac{\pi fk\sigma^2}{z^2+k^2\sigma^4}}\right)^2 \\[2ex]
& +4e^{\frac{\pi fk\sigma^2}{z^2+k^2\sigma^4}} sin^2\left(\frac{f\pi/2}{1+\left(k\sigma^2/z\right)^2}\right) \Bigg]. \qquad (8)
\end{aligned}
$$

where we have considered that different points along the perimeter of a ring are uncorrelated, $C=0$.

The limit $C=0$ means that two joint points of the edge of the ring are uncorrelated. It happens, for example, when the lens is engraved pixel by pixel or line by line, as a printer does. We show in Fig. 2 the intensity along axis calculated with Equation 8 corresponding to different amounts of roughness in the edges. As can be observed, the secondary foci disappear for a certain amount
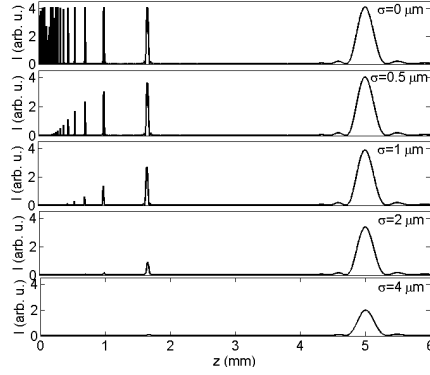
Figure 2: Theoretical intensity along the optical axis calculated with Equation 8 for different amounts of roughness in the edges of the zones of a FZP with the following parameters: $D \approx 400~\mu m$, $\lambda = 630~nm$, $f = 5~mm$, and $C = 0~\mu m$.

of roughness. Despite primary focus decays to a half for this case, it is the only one that survives for a certain roughness forward. Therefore, random edges on binary amplitude FZPs make them single-focus lenses, cancelling diffractive effects.

In addition, we show in Fig. 3 the evolution of the four main foci in terms of the roughness of the edges. For a FZP of focal length $f = 5~mm$ and diameter $D = 400~\mu m$ all secondary foci decays almost to zero intensity for $\sigma = 3~\mu m$. There are more secondary foci that goes to zero before the foci shown in Fig. 3 but we do not show them into the figure for clearness. Anyway, for $\sigma = 2~\mu m$ the secondary foci decrease to a 5% and the primary focus still has around 50% of the intensity with respect of the non-rough FZP.
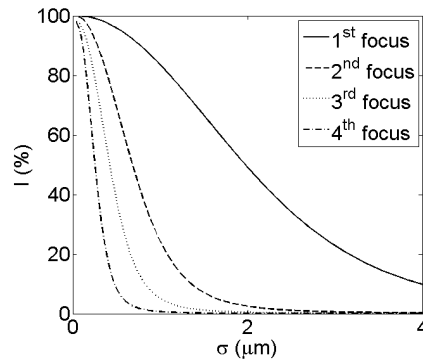

Figure 3: Evolution of the main foci intensity in terms of the roughness of the edges of a FZP with the following parameters: $D \approx 400~\mu m$, $\lambda = 630~nm$, $f = 5~mm$, and $C = 0~\mu m$.

3. Numerical simulations

Following, to corroborate the analytical results we have performed a numerical simulation using a fast-Fourier transform based direct integration method that uses the Rayleigh-Sommerfeld approach, [20]. Besides, this method allows investigating the behavior of the FZP out of axis. Firstly, we define the lens as an ensemble of concentric rings with a certain amount of edge roughness in the same fashion as Fig. 1. The intensity along the optical axis calculated numerically for the same parameters as Fig. 2 is shown in Fig. 4. Foci result slightly wider than for the analytical approach due to numerical issues and truncations. Besides, it is less sampled since we have used fewer points than for the analytical approach due to numerical and computational memory restrictions. This is the reason why secondary foci do not appear clearly in Fig. 4.
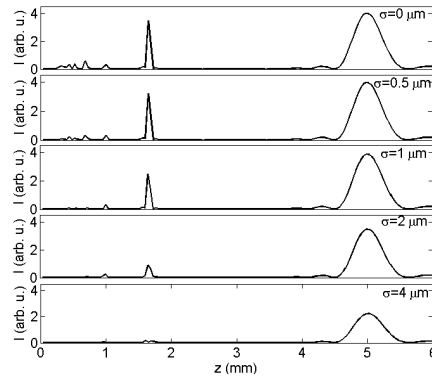

Figure 4: Intensity along optical axis calculated numerically for different amounts of roughness in a FZP with the following parameters: $D \approx 400\ \mu m$, $\lambda = 630\ nm$, $f = 5\ mm$, and $C = 0\ \mu m$.

Anyway, numerical simulations clearly corroborate the theoretical approach. On the other hand, despite the random edges and the disappearance of secondary foci, the propagating intensity does not accumulate noise as can be observed in Fig. 5 and Fig. 6. We show the intensity profile for $\sigma = 0\ \mu m$ and $\sigma = 4\ \mu m$, Fig. 5. The power of the main focus decreases but its shape remains, making it still valid for applications, Fig. 6.

4. Experimental verification

Finally, we have performed an experiment using a He-Ne laser ($\lambda = 638\ nm$), a Spatial Light Modulator (SLM) model LC-R 2500 by HoloEye, (pixel size of 19 μm, resolution 1024x798 pixels) and a CMOS camera model DMx 72BUC02 by Imaging Source (pixel size $2.2 \times 2.2\ \mu m$). The experiment consists of imprinting the designed FZP into the amplitude configured SLM and taking the intensity with the CMOS camera moving it along the optical axis by using a motorized linear stage. We show in Fig. 7 the intensity along the optical axis around the principal and secondary focus for a FZP of diameter 9.7 mm, focal
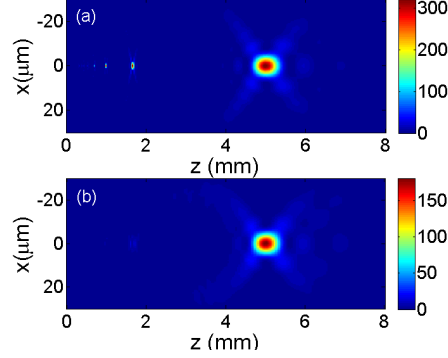
Figure 5: Numerical intensity profile propagation of a FZP with the following parameters: $D \approx 400 \ \mu m$, $\lambda = 630 \ nm$, $f = 5 \ mm$, and $C = 0 \ \mu m$. (a) $\sigma = 0 \ \mu m$ and (b) $\sigma = 4 \ \mu m$.
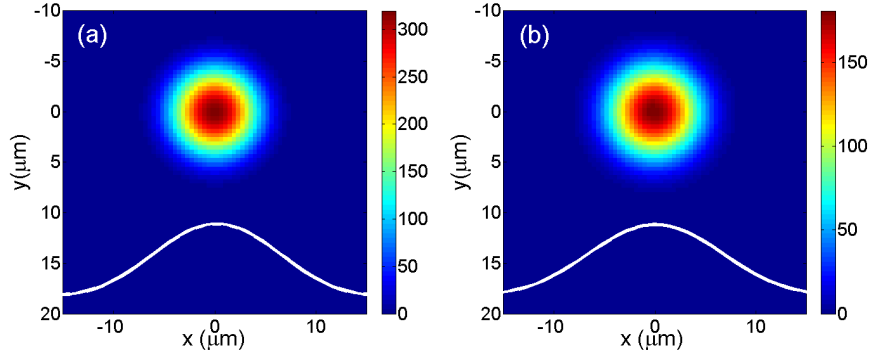

Figure 6: Intensity at the primary focus of a FZP of diameter $D \approx 400 \ \mu m$ focal length $f = 5 \ mm$ and correlation coefficient $C = 0 \ \mu m$ calculated numerically considering a plane wave of $\lambda = 630 \ nm$. (a) $\sigma = 0 \ \mu m$ and (b) $\sigma = 4 \ \mu m$.

length $f = 33 \ mm$, and two amounts of roughness. The displacement of the foci due to the random edges with respect of its nominal position is also experimentally observed. In addition, we show in Fig. 8 an image of the experimental focal spot without, Fig. 8a, and with rough edges, Fig. 8b. Both are very similar and roughness in the zones edges do not affect to the focusing properties of the primary focus except for a decreasing in contrast.

Conclusions

Summarizing, a kind of binary amplitude Fresnel zone plate with single focus has been proposed and analyzed. It consists of a Fresnel zone plate with random roughness at the edges of the different zones. We theoretically, numerically, and experimentally demonstrate how this kind of lens cancels secondary foci inherent to Fresnel zone plates. The developed formalism can be easily extended to binary
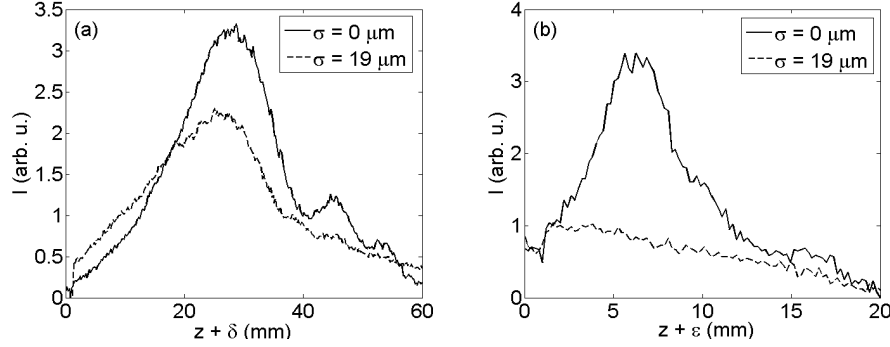
Figure 7: Experimental intensity along axis around the principal focus (a) and the secondary focus (b) for a FZP with the following parameters: $D \approx 9.7\ mm$, $\lambda = 632.8\ nm$, $f = 33\ mm$, $C = 0\ \mu m$, and different amounts of randomness: $\sigma = 0\ \mu m$ (solid line) and $\sigma = 19\ \mu m$ (dashed line). δ and ϵ are unknown constants dependent on the initial position of the linear stage used for displacing the camera.

phase Fresnel zone plates and, aside from the theoretical interest, this kind of zone plates can be useful in a wide range of photonic applications that can also involve soft and hard X-rays or extreme ultra-violet radiation.

Acknowledgments

[1] Hecht E 1998 *Optics, 4th Edition, Addison Wesley Longman Inc, 1998*

[2] Saavedra G, Furlan W D and Monsoriu J A 2003 *Optics letters* **28** 971–973

[3] Wang X, Xie Z, Sun W, Feng S, Cui Y, Ye J and Zhang Y 2013 *Optics letters* **38** 4731–4734

[4] Salgado-Remacha F J, Sanchez-Brea L M, Alvarez-Rios F J and Bernabeu E 2010 *Applied optics* **49** 1750–1756

[5] Alda J, Rico-García J M, Salgado-Remacha F J and Sanchez-Brea L M 2009 *Optics Communications* **282** 3402–3407

[6] Zhang B, Zhao D and Wang S 2007 *Applied physics letters* **91** 021108

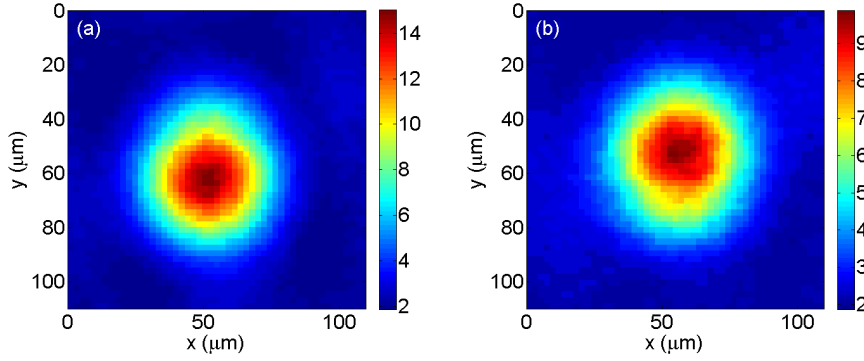[7] Di Fabrizio E, Romanato F, Gentili M, Cabrini S, Kaulich B, Susini J and Barrett R 1999 *Nature* **401** 895–898

Figure 8: Experimental intensity at the primary focus of a FZP with the following parameters: $D \approx 9.7$ mm, $f = 33$ mm, $C = 0$ μm and a laser of a lens of focal length $\lambda = 632.8$ nm considering (a) $\sigma = 0$ μm and (b) $\sigma = 19$ μm.

[8] Kim H C, Ko H and Cheng M 2009 *Optics express* **17** 3078–3083

[9] Fu Y, Zhou W and Lim L E N 2008 *JOSA A* **25** 238–249

[10] Quiney H, Peele A, Cai Z, Paterson D and Nugent K 2006 *Nature Physics* **2** 101–104

[11] Judd T, Scott R, Sinuco G, Montgomery T, Martin A, Krüger P and Fromhold T 2010 *New Journal of Physics* **12** 063033

[12] Hristov H D 2000 *Fresnal Zones in Wireless Links, Zone Plate Lenses and Antennas* (Artech House, Inc.)

[13] Lai B, Yun W, Legnini D, Xiao Y, Chrzas J, Viccaro P, White V, Bajikar S, Denton D, Cerrina F *et al.* 1992 *Applied physics letters* **61** 1877–1879

[14] Chu Y, Yi J, De Carlo F, Shen Q, Lee W K, Wu H, Wang C, Wang J, Liu C, Wang C *et al.* 2008 *Applied Physics Letters* **92** 103119

[15] Srisungsitthisunti P, Ersoy O K and Xu X 2007 *Applied physics letters* **90** 011104

[16] Kipp L, Skibowski M, Johnson R, Berndt R, Adelung R, Harm S and Seemann R 2001 *Nature* **414** 184–188

[17] Beynon T, Kirk I and Mathews T 1992 *Optics letters* **17** 544–546

[18] Goodman J W 2015 *Statistical optics* (John Wiley & Sons)

[19] Teng S, Cui Y and Li Z 2015 *Journal of Optics* **18** 015601

[20] Shen F and Wang A 2006 *Applied optics* **45** 1102–1110